J. Iran. Chem. Soc., Vol. 5, No. 3, September 2008, pp. 367-374.

JOURNAL OF THE
Iranian
Chemical Society

A Credible Role of Copper Oxide on Structure of Nanocrystalline Mesoporous Titanium Dioxide

S. Rahimnejad, S. Rahman Setayesh and M.R. Gholami*
Department of Chemistry, Sharif University of Technology, Azadi Ave., P.O. Box 11365-9516, Tehran, Iran

(Received 7 April 2007, Accepted 22 May 2007)

Copper oxide-titania catalysts with nanocrystalline mesoporous structure were prepared by sol-gel technique using tetra isopropyl *ortho* titanate (TiPT) as the inorganic precursor and amino-2 ethanol as the swelling agent. Characterization was performed using X-ray diffraction (XRD), fourier transformed infrared spectra (FTIR), scanning electron microscopy (SEM), diffuse reflectance UV-Vis spectroscopy (DRS), and N_2 adsorption-desorption measurements. It was found that CuO (0.025-0.1 mol ratio) has some effect on the particle size, surface area, pore-volume, pore-diameter, crystallinity of the particles, and crystalline phase of TiO_2 nanocrystalline. The results indicated that 0.1 CuO-TiO_2 had higher surface area and total pore volume among all CuO-TiO_2 samples. The S_{BET} value of 0.1 mol ratio CuO-load TiO_2 sample is approximately similar to that of Degussa P25 while its pore volume (0.1198 $cm^3\ g^{-1}$) is larger than Degussa P25 due to production of large number of pores. Therefore, the physical property of 0.1 CuO-TiO_2 catalyst is comparable with Degussa P25.At 823K, the 0.1 mol ratio CuO-load TiO_2 sample shows the phase transformation from anatase to rutile in the ratio of 1:1.1. The synthesized CuO-TiO_2 nanocrystalline will be able to show photocatalytic reaction under visible light.

Keywords: TiO_2, CuO, Mesoporous, Nanocrystalline

INTRODUCTION

Photocatalysis is a process in which a photocatalyst material simultaneously absorbs efficient photons and reactants. A photocatalyst upon absorption of photons whose energy is equal to or greater than their band-gap energy, an electron-hole pairs is created, which dissociates into free photo electrodes in the conduction band and photo holes in the valance band. According to the redox potential of each adsorbate, photoelectrons are transferred to acceptor molecules, where act as positive photoholes to donor molecules. Among various photocatalysts, titanium dioxide is frequently used due to its high photocatalytic activity, biological and chemical inertness, thermal stability, non-corrosive properties, and non-toxicity.

Large surface area titanium dioxide with nanosized particles or mesostructure has been receiving much attention for its application in different areas including gas sensing, photocatalysis, photoelectrodes, solar energy conversion and water splitting to produce hydrogen. The anatase phase has a higher photocatalytic and photoelectrical conversion activity than amorphous, rutile and brookite phases. Therefore, mesoporous TiO_2 containing the high crystallization of anatase has attracted much attention due to its high surface area and a passage wide enough for the ingress of reactants and egress of product, which enhances the surface reactions [1-4].

It was reported that transition metal ions doping (*e.g.*, Fe^{3+}) can enhance the photocatalytic activity of TiO_2 [5]. Copper

---

*Corresponding author. E-mail: Gholami@sharif.edu oxide has been extensively studied as an important component of CuO superconductors because of being a p-type semiconductor. With regard to its commercial value and semiconductor properties, CuO has also been widely exploited as a powerful heterogenous catalyst [6-15], photocatalyst [16-20], magnetic storage medium, solar energy transformer and gas sensor [21,22].

Therefore, the synthesis of CuO-loaded mesoporous titanium dioxide nanocrystalline seems to be valuable for heterogenous photocatalysts. In this study, the CuO loaded mesoporous nanocrystalline powder photocatalyst was prepared *via* the sol-gel technique. The particle size, crystallinity of the particles, surface area, pore-volume, pore-diameter and the phase transformation from anatase to rutile were reported.

EXPERIMENTAL

Material

Tetra isopropyl *ortho* titanate was supplied from Merck and was used without further purification.

Catalysts Preparation

CuO-loaded mesoporous TiO_2 nanocrystalline photocatalysts were prepared by the sol-gel technique. Tetraisopropyl *ortho* titanate and amino-2 ethanol were dissolved in ethanol. Following vigorous stirring for 2 h at room temperature, a mixed solution of water and ethanol was added drop wise to the above solution with a pipette under stirring. The chemical composition of the starting alkoxide solution was 1:1:26.5:5 in molar ratio ($C_{12}H_{28}0_4Ti$:H_2O: C_2H_5OH:$C_4H_{11}NO_2$). Finally, various amounts of copper acetate ($Cu(CH_3COO)_2.H_2O$) solution in ethanol were added to the above precursor titanium sol. The resultant mixture was stirred for 2.5 h and then aged several days at room temperature to become gel. The gel was heated at 353-373 K to evaporate solvent and then calcined at 823 K for 6 h in the furnace under static air to remove organic substances.

Catalysts Characterization

The X-ray diffraction (XRD) patterns were obtained with a D_4 ENDEAVOR Bruker diffractometer using Cu Kα radiation ($\lambda = 0.15406$ nm). The crystallite size was estimated from the broadening of the diffraction peaks employing the Scherrer equation: $D = 0.89\ \lambda/\beta \cos\theta$, where D is the crystallite size, λ is the wavelength of the X-ray radiation ($\lambda = 0.15406$ A°), β is the peak width at half-maximum height ($2\theta = 25.3°$) for anatase (101), and 0.89 is the Scherrer constant. Scanning electron microscopy (SEM) of the samples was carried out using a Philips XN 30 instrument and the average particle size was estimated by SEM. Fourier transform infrared (FTIR) spectra in the range of 4000-400 cm^{-1} were recorded on a ABB BOMEM MB series spectrophotometer. The samples for FTIR were prepared using the KBr technology. Diffuse reflectance UV-Vis spectroscopy was performed using a Cintra 40 instrument with $BaSO_4$ as the standard. The Brunauer-Emmett-Teller (BET) surface areas of the samples were analyzed by nitrogen adsorption in a BELSORB nitrogen adsorption apparatus. The BET surface area was calculated by multipoint BET method. The adsorption isotherm was also used to determine the pore size distribution using the Barret-Joyyner-Halender (BJH) method. The nitrogen adsorption volume at the relative pressure (p/p^o) of 0.988 was used to measure the pore volume and average pore size of the samples.

RESULTS AND DISCUSSION

The X-ray powder diffraction was used to determine the crystalline phases present in the prepared CuO-loaded and un-loaded mesoporous nanocrystalline TiO_2. Figure1 shows the effect of CuO concentration on phase structures of nanocrystalline TiO_2 prepared by the sol-gel technique. Comparsion of the X-ray diffractogram with JCPDS files demonstrates that TiO_2 anatase and rutile were the phases present in all samples. It can be seen that the phase transformation of TiO_2 occurred in the CuO-TiO_2 catalysts calcined at 823 K; in 0.1 CuO-TiO_2, the rutile phase was more than anatase phase. In Fig. 1, peaks marked "A" and "R" correspond to anatase and rutile phases, respectively. The amount of CuO loading does not have any effect on the crystallization of TiO_2. The high density of surface defects in 0.1 CuO-TiO_2 may be used to explain the phase transformation of anatase to rutile. Furthermore, the patterns indicated that CuO-TiO_2 samples consisted of relatively small crystallite size in the average range of 19.5 nm, which was estimated by line broadening of anatase (101) diffraction peak.

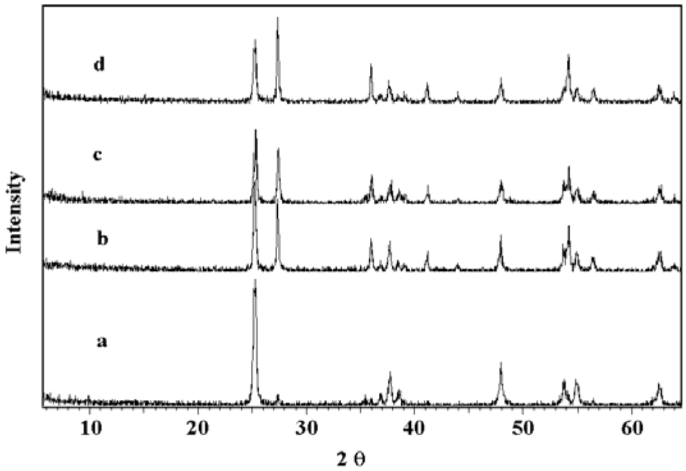

Fig. 1. XRD patterns of different CuO-loaded TiO_2: (a) 0.025 CuO-TiO_2, (b) 0.033 CuO-TiO_2, (c) 0.05 CuO-TiO_2, (d) 0.1 CuO-TiO_2.

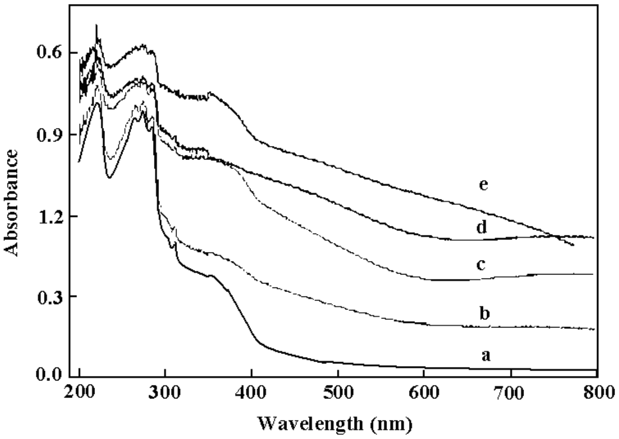

Fig. 2. DRS Spectra of (a) TiO_2, (b) 0.025 CuO-TiO_2, (c) 0.033 CuO-TiO_2, (d) 0.05 CuO-TiO_2, (e) 0.1 CuO-TiO_2.

It can be realized that samples with different amounts of copper oxide loaded on titanium dioxide have approximately the same crystalline size, so that it can be concluded that copper oxide has not doped on titanium dioxide crystal lattice. In fact, titanium dioxide has only plays the role of a support for copper oxide.

Since UV-Vis light excitation creates photo-generated electrons and holes, the UV-Vis diffuse reflectance spectroscopy was used to probe the band structure and molecular energy levels in the crystal. Figure 2 represents the DRS absorption spectra of nanocrystalline TiO_2 (a) and CuO loaded TiO_2 of mol ratios of 0.025 (b), 0.033 (c), 0.05 (d) and 0.1 (e). The UV-absorption edge of nanocrystalline TiO_2 appeared at about 430 nm. It is observed that the UV-absorption edge of the CuO loaded TiO_2 was extended to longer wavelength (red shift). This result indicates that the copper oxide with a narrow band gap (1.4) increased the visible light adsorption ability of TiO_2. The CuO loaded TiO_2 had trapping level which decrease the TiO_2 band gap (Eg).

According to the quantum size effect, the band gap energy

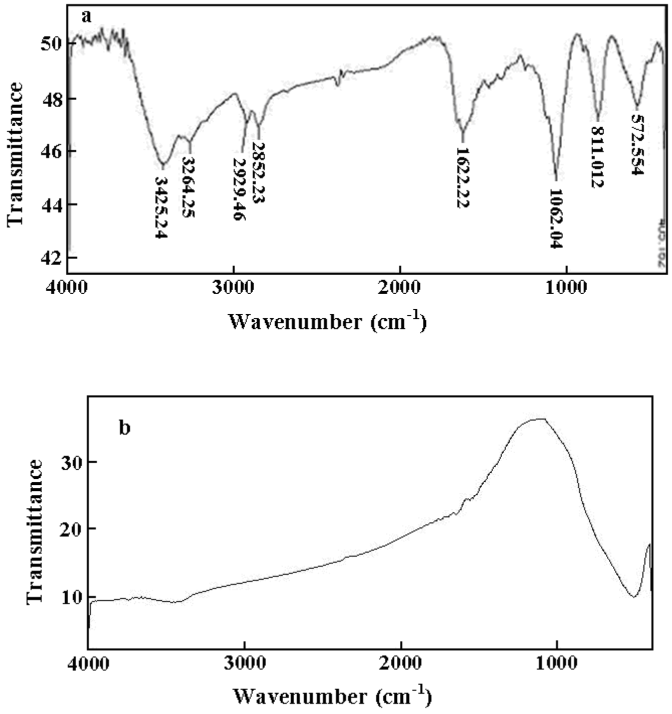

Fig. 3. FT-IR Spectra of uncalcined (a) CuO-TiO_2 and (b) calcined CuO-TiO_2 catalyst at 823 k for 3 h.

is expected to increase (blue shift) with decreasing particle size. However, the results are in contrast to this effect due to the presence of CuO. The most possible mechanism for the observed absorption might involve oxygen vacancies produced by different loaded CuO, which form localization levels in the range of 400-800 nm. Therefore, the synthesized nanocrystal will be able to show photocatalytic reaction under visible light.

Figure 3a shows the representative IR spectra (4000-400 cm^{-1}) where OH groups can be observed. In the prepared gel, the 3200 cm^{-1} band has to be attributed to hydroxyl groups (Ti-OH) and to OH from water, ethanol, and amino-2 ethanol which are occluded in the titania pore. The OH bending band of water in the gel is observed at 1650 cm^{-1} and the low energy interval the Ti-O bond bands are found at 1061 and below 1000 cm^{-1}. When the catalyst was calcined at 823 K (Fig. 3b) the high energy stretching band almost fades and the 1600 cm^{-1} bending vibration band intensity decreases due to vaporization of the liquid. In the low energy interval, the band at 550 cm^{-1} is due to stretching vibrations Ti-O and Cu-O and the broad bands between 800 and 1400 cm^{-1} are attributed to the lattice vibrations of titanium oxide. It should be noted that no traces of solvents such as aminoethanol, ethanol and water have been observed in calcined oxide catalyst.

Representative N_2 adsorption-desorption isotherms of CuO-loaded TiO_2 samples are depicted in Fig. 4. The isotherms of all samples exhibited typical type IV with H1 and H2 hystersis loop according to IUPAC classification. The apparent step in the adsorption branch with the sharp decline in desorption branch were identified at a relative pressures (p/p^o) approximately between 0.5 and 0.9 which is an indication of mesoporosity.

Figure 5 represents pore size distribution curve calculated from the adsorption branch of the isotherms by the BJH method. The BET surface areas and pore parameters of the samples are summarized in Table 1. The 0.1 mol ratio CuO-loaded TiO_2 showed larger S_{BET} and total pore volume than the other loadings and pure TiO_2. This may be attributed to the fact that CuO loaded at 0.1 mol ratio concentration inhibited the growth of nanocrystalline TiO_2. The diameter range of pores was from 2-10 nm in all samples. The average pore

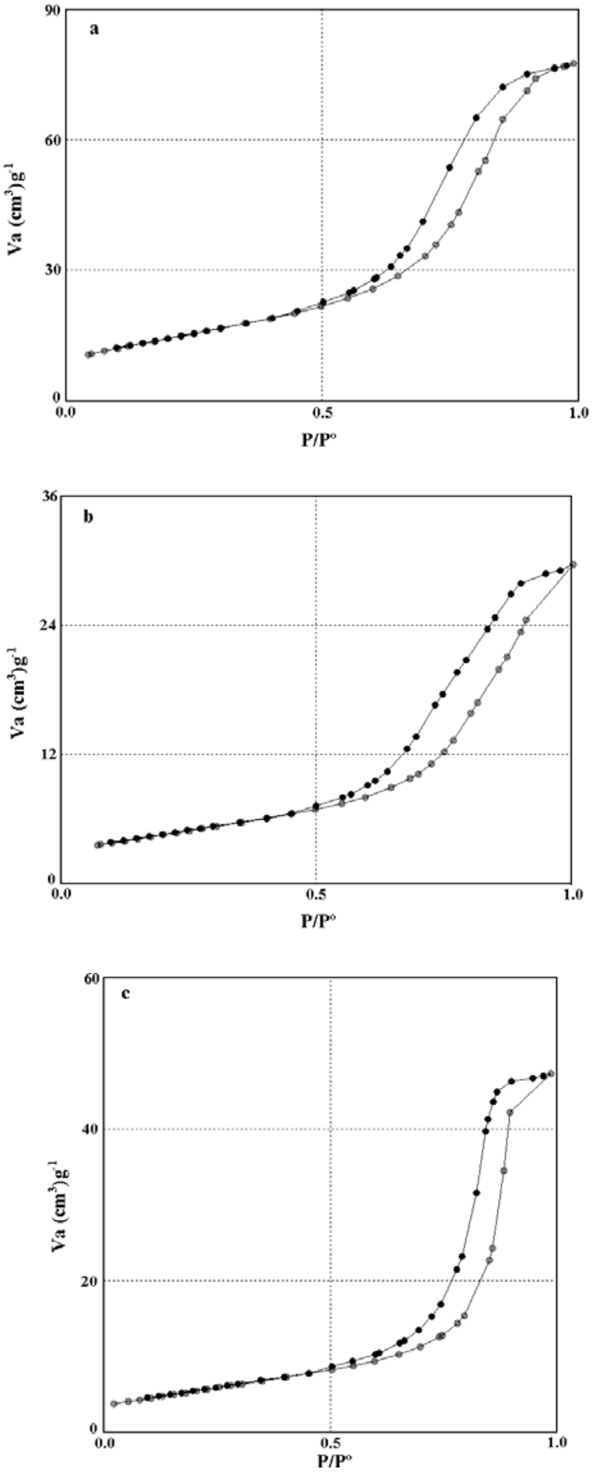

Fig. 4. The adsorption and desorption isotherms of N_2 at 77 K on CuO-loaded TiO_2 nanocrystalline samples: (a) 0.025, (b) 0.033, (c) 0.1.

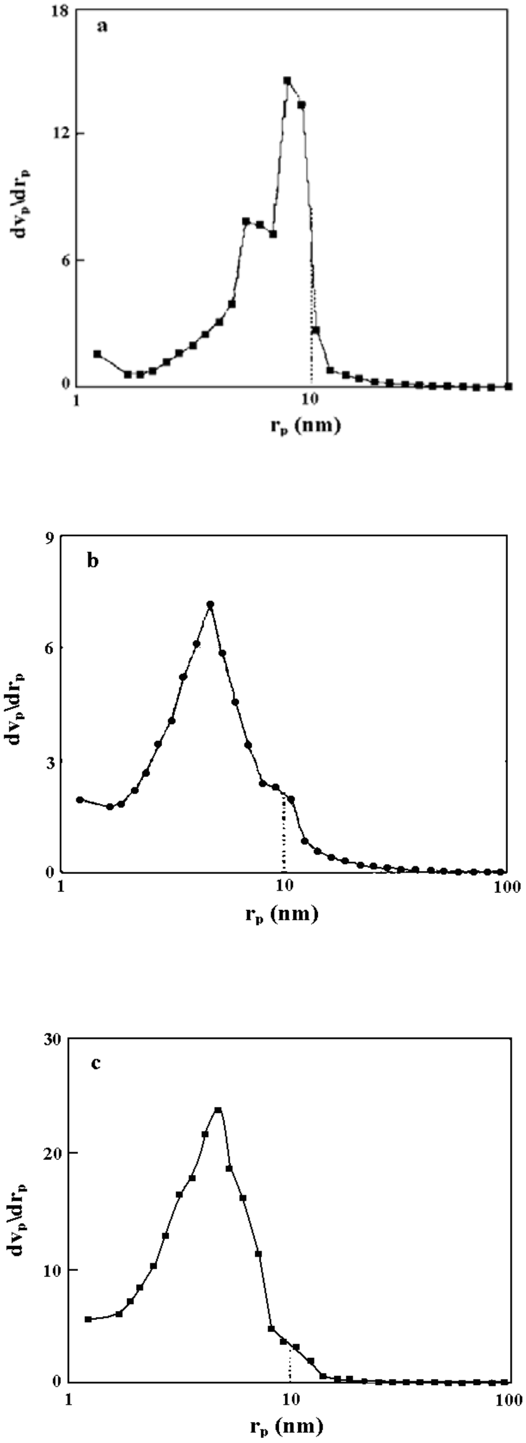

Fig. 5. Pore Size distribution (BJH) of CuO loaded TiO_2 nanocrystalline: (a) 0.025, (b) 0.033, (c) 0.1.

Table1. Textural Properties from N_2 Adsorption-Desorption Isotherm Measurement of CuO-Loaded TiO_2

Catalyst	$RCuO/TiO_2$	BET surface area ($m^2\ g^{-1}$)^a	Mean pore diameter (nm)	Total pore volume ($cm^3\ g^{-1}$)^b
P25-Degussa[c]	-	63.0	3.8	0.060
TiO_2	-	28.61	30.44	0.2177
A	0.025	20.28	14.43	0.073
B	0.033	17.58	10.73	0.046
C	0.1	51.62	9.28	0.1198

[a] BET surface area calculated from the linear part of the BET plot (p/p° = 0.07-0.5). [b] Total pore volume, taken from the volume of N_2 adsorbed at about p/p° = 0.98. [c] See Ref. [5].

diameter of samples was about 9.3-14.4 nm, which again confirmed the mesoporous structure (see Table 1). Pore size distribution (BJH) showed that the increased concentration of CuO loading will result in decreased average pore size (Table 1). There are two possible factors causing the decrease in average pore size. One is that the smaller crystallite aggregation forms smaller pores. The second is that some loading CuO insert into the pore of mesoporous TiO_2 powders result in smaller pore size.

Figure 6 shows the SEM micrographs of the different CuO loaded TiO_2 prepared by hydrolysis of tetraisopropyl *ortho* titanate and calcined at 823 K for 3 h. In all micrographs, the TiO_2 particles can be observed as aggregated clusters consisting of many nanoparticles. It is obvious that as the amount of loaded CuO increases, the TiO_2 particles become larger and also the total pore volume will increase.

CONCLUSIONS

We managed to prepare CuO loaded TiO_2 with mesoporous nanocrystalline structure by single step sol-gel method. CuO loading influenced the phase transformation of anatase to rutile. The ratio of rutile to anatase was the highest in 0.1 CuO-TiO_2. The 0.1 CuO loaded TiO_2 sample had larger specific surface area and total pore volume (close to P25). CuO loading increased the porosity of TiO_2, while did not have any effect on the crystallite size. The photocatalytic activity of CuO-load mesoporous nanocrystalline TiO_2 can be higher than TiO_2 due to lower band gap.

ACKNOWLEDGEMENTS

The authors are grateful to the Sharif University of Technology for financial support. They have also special appreciation to Dr. N. Taghavinia, Physics Department at Sharif University of Technology.

REFERENCES

[1] M. Alvaro, C. Aprile, M. Benitez, E. Carbonell, H. Garcia, J. Phys. Chem. B 110 (2006) 6661.
[2] B.L. Bischoff, M.A. Anderson, Chem. Mater. 7 (1995) 1772.
[3] Y. Wang, S. Zhang, X. Wu, Nanotech. 15 (2004) 1162.
[4] X. Yu, Y. Li, W. Ge, Q. Yang, N. Zhu, K. Kalantar-Zadeh, Nanotech. 17 (2006) 808.
[5] M. Zhou, J. Yu, B. Cheng, H. Yu, Mater. Chem. Phys. 93 (2005) 159
[6] L. Wang, A. Kong, B. Chen, H. Ding, Y. Shan, M. He, J. Mol. Catal. A 230 (2005) 143.
[7] L.N. Franco, I.H. Perez, J.A. Pliego, A.M. Franco, Catal. Today 75 (2002) 189.
[8] S. Valange, Z. Gabelica, M. Abdellaoui, J.M. Clacens, J. Barranlt, Micropor. Mesopor. Mater. 30 (1999) 177.
[9] B. Chou, J.L. Tsai, S. Cheng, Micropor. Mesopor. Mater. 48 (2001) 309.
[10] X. Hu, F.L.Y. Lan, L.M. Chaung, K.F. Chan, X.S. Zhao, G.Q. Lu, Catal. Today 68 (2001) 129.
[11] B. Chou, J.-L. Tsai, S. Cheng, Micropor. Mesopor.

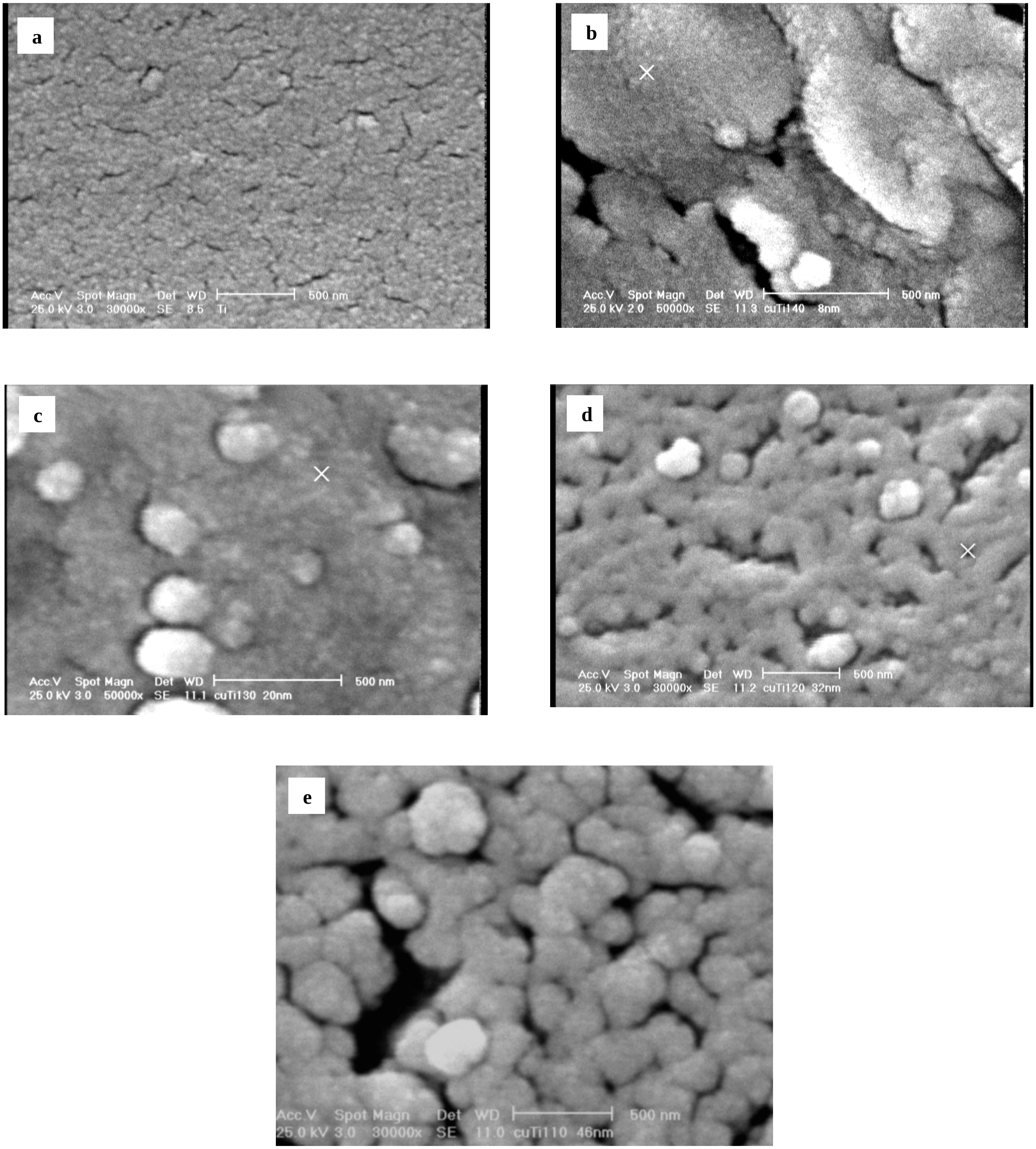

Fig. 6. SEM image of different CuO-loaded TiO_2 samples: (a) pure TiO_2, (b) 0.025, (c) 0.033, (d) 0.05, (e) 0.1.

Mater. 48 (2001) 309.

[12] X. Bokhimi, A. Morales, O. Novaro, Chem. Mater. 9 (1997) 2616.

[13] H. Zhu, Y. Wu, X. Zhao, H. Wan, L Yang, J. Hong, Q. Yu, L. Dong, Y. Chen, C. Jian, J. Wei, P. Xu, J. Mol. Catal. A 243 (2006) 24.

[14] S. Suarez, J.A. Martin, M. Yates, P. Avila, J. Blanco, J. Catal. 229 (2005) 227.

[15] S. Velu, L. Wang, M. Okazaki, K. Suzuki, S. Tomura, Micropor. Mesopor. Mater 54 (2002) 113.

[16] K. Chiang, R. Amal, T. Tran, Adv. Envir. Res. 6 (2002) 471.

[17] Slamet, H.W. Nasution, E. Purnama, S. Kosela, J. Gunlazuardi, Catal. Commun. 6 (2005) 313.

[18] J.C.S. Wu, H.-M. Lin, C.-L. Lai, Appl. Catal. A 296 (2005) 194.

[19] T. Sreethawong, S.Y. Oshikawa, Catal. Commun. 6 (2005) 661

[20] S. Li, H. Zhang, Y. Ji, D. Yang, Nanotech. 15 (2004) 1428.

[21] W. Wang, O.K. Varghese, C. Ruan, M. Paulose, G.A. Grimes, J. Mater. Res. 18 (2003) 2756.

[22] Z. Wang, W. Cai, X. Hong, X. Zhao, F. Xu, C.H. Cai, Appl. Catal. B 57 (2005) 223.